nature neuroscience

An independent, landmark-dominated head-direction signal in dysgranular retrosplenial cortex

Pierre-Yves Jacob[1], Giulio Casali[1], Laure Spieser[2], Hector Page[1], Dorothy Overington[1] & Kate Jeffery[1]

We investigated how landmarks influence the brain's computation of head direction and found that in a bidirectionally symmetrical environment, some neurons in dysgranular retrosplenial cortex showed bidirectional firing patterns. This indicates dominance of neural activity by local environmental cues even when these conflicted with the global head direction signal. It suggests a mechanism for associating landmarks to or dissociating them from the head direction signal, according to their directional stability and/or utility.

The sense of direction is computed by head direction (HD) cells[1], which fire when the animal faces a particular direction. The HD signal is derived from learned environmental landmarks[2], but the brain needs to know that these are spatially stable before it can use them as directional markers[3]. This circular problem thus requires interplay between the existing directional representation and newly encountered landmarks. We investigated the hypothesis that retrosplenial cortex (RSC), a HD structure that processes landmark stability[4], is involved in this interplay process. RSC is a cortical region[5–7] that is directly connected to visual cortex as well as to the main HD network[8]. We exposed rats to an environment where global and local directional cues were in conflict and recorded RSC neurons, as well as HD cells from anterior thalamus and postsubiculum. Rats freely moved between two connected, rectangular compartments (**Supplementary Fig. 1**). Each compartment contained landmarks that were reversed in orientation relative to those in the other, thus dissociating local landmarks and global direction. To orient the global HD system, the symmetry of the apparatus was broken by scenting one compartment with lemon and the other with vanilla.

Of 1,090 RSC neurons (**Supplementary Table 1**), we identified 96 classic HD cells (9%), each with a single tuning curve that maintained a constant direction across compartments and thus reversed its relation to the local cues depending on odor context (**Fig. 1a**, **Supplementary Fig. 2** and **Supplementary Table 2**). This confirmed that HD cells can use odor-context information to resolve spatial ambiguity. However, many neurons had two opposing HD tuning curves (**Fig. 1b** and **Supplementary Fig. 3**). We derived a measure of such bidirectional firing to identify 116 of these bidirectional (BD) cells (11%) (**Supplementary Fig. 4**) and undertook several analyses to rule out that the bidirectional pattern could have been recording artifact (**Supplementary Fig. 5**). Moreover, many BD cells showed compartment-specific activity (see below), meaning that the individual cells

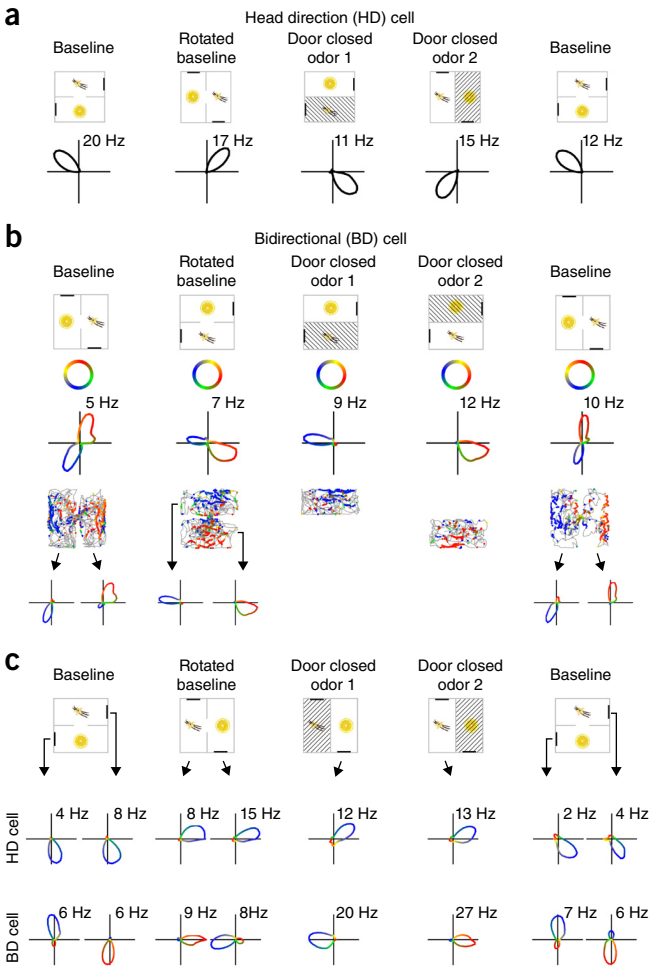

Figure 1 Two types of directional encoding by RSC neurons. (**a**) Example of an RSC HD cell. Top: Orientation of the apparatus (cross-hatching indicates unavailable compartments). Bottom: polar plots of firing rate vs. head direction (numbers indicate the peak rate). (**b**) Example of an RSC BD cell. Tuning curves (third row) are color-coded according to the color key (second row). Fourth row: directional color-coding of action potentials, superimposed on the animal's path (grey), reveals the compartment-specificity of firing directions. Bottom row: tuning curves from each subcompartment in isolation. (**c**) Simultaneous recordings of a BD cell and a classic (unidirectional) HD cell, color-coded as in **b**, revealing the dissociation in tuning curve direction.

[1]Institute of Behavioural Neuroscience, Research Department of Experimental Psychology, Division of Psychology and Language Sciences, University College London, London, UK. [2]Department of Psychology, City University of London, London, UK. Correspondence should be addressed to K.J. (k.jeffery@ucl.ac.uk).

Received 1 August; accepted 21 November; published online 19 December 2016; doi:10.1038/nn.4465

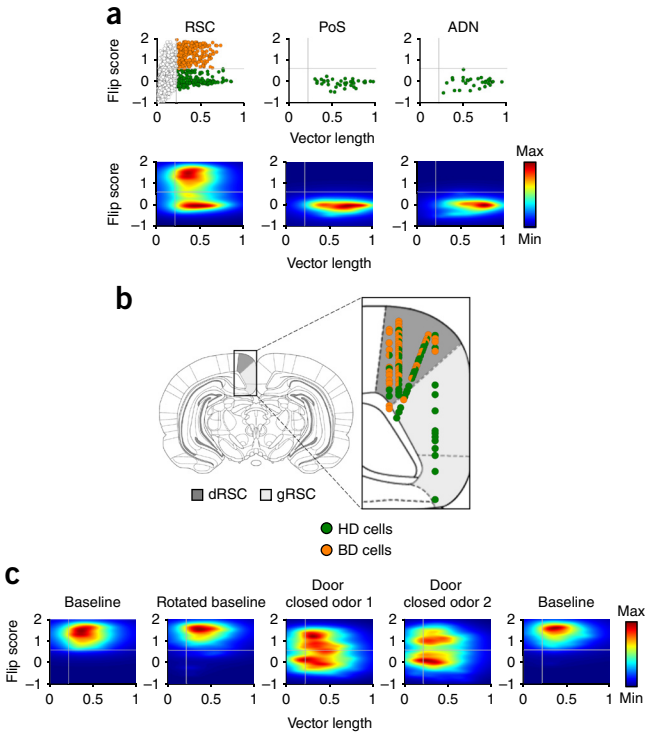

Figure 2 BD cells are specific to dysgranular RSC. (**a**) Distribution of bidirectional firing patterns (flip score) as a function of directional tuning (calculated as angle-doubled Rayleigh vector length; Online Methods) for 1,090 RSC cells and for postsubiculum (PoS) and anterior thalamus (ADN) cells in trial 1. Gray lines show the Rayleigh vector and flip score thresholds for determining all directional cells and BD cells, respectively. Top: scatter plot showing BD cells (orange) and HD cells (green). Bottom: density plots of the same data revealing two clear populations. (**b**) Recording sites of BD (orange) and HD (green) cells within the dysgranular (dRSC, dark gray) and granular (gRSC, light gray) RSC. (**c**) Density plots of RSC BD cells across 5 recording trials, collapsed across cells/sessions. Note that some cells became unidirectional (with a low flip score) when the door closed.

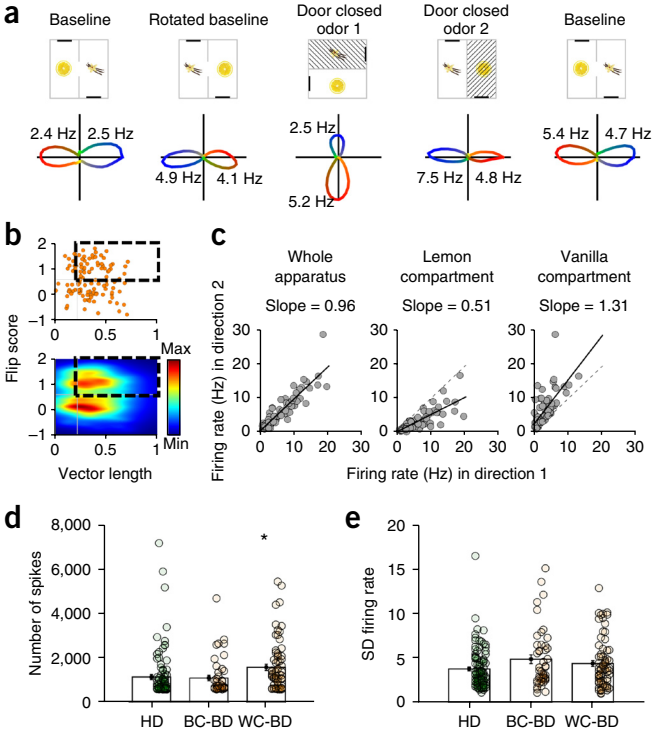

Figure 3 WC-BD activity. (**a**) Example of a WC-BD cell. (**b**) 70/116 (60%) showed within-compartmental bidirectionality. (**c**) Size asymmetry of tuning curves in the WC-BD cells is compartment-specific. Direction 1 was defined as the direction of the biggest peak in the lemon compartment and direction 2 as the direction opposite to that. Overall, firing rates were similar in the two compartments (left), but the direction of the dominant peak reversed between compartments. (**d**,**e**). Analysis of spike count (**d**) revealed an increase in spiking for WC-BD cells (1,557.49 ± 41.86) compared with BC-BD cells (1,058.93 ± 128.75) and HD cells (1,041.26 ± 117.65); one-way ANOVA: $F_{2,209} = 5.00$, $P = 0.01$; $^*P < 0.05$. However, firing-rate spread, measured as the standard deviation (s.d.) of firing rates (**e**), was not different between cell types, being 3.80 ± 0.23 for HD cells, 4.90 ± 0.49 for BC-BD cells and 4.41 ± 0.33 for WC-BD cells ($F_{2,209} = 2.80$, $P = 0.07$). Solid lines show mean ± s.e.m.

in the putative cell-pairs would have to have fired in only one compartment, which has never been observed in HD cells.

Forty-six of the BD neurons were compartment-specific (**Fig. 1b** and **Supplementary Fig. 3**), meaning that the cells actually had unidirectional firing that reversed each time the rat passed through the doorway, producing a bidirectional pattern overall. This was shown by analyzing cell firing activity in each compartment separately and also by closing the door, after which tuning curves became unidirectional (**Fig. 1b**). This reversal between compartments meant that the tuning curves maintained the same relationship to the local landmarks. BD cells were recorded simultaneously with the non-reversing HD cells (**Fig. 1c** and **Supplementary Fig. 6**), such that BD and HD cells dissociated their responses when the rat changed compartments. BD cells also followed apparatus rotation more reliably than HD cells (**Supplementary Fig. 7**). Thus, a population of RSC neurons was dissociable from the main HD network and was dominated by landmarks, an observation that refutes the previous belief that the entire HD network is coherent[9,10].

We looked for bidirectional firing in two other HD-cell regions, postsubiculum and the anterior thalamus, but in these regions we found only classic HD cells (**Fig. 2a**). In addition, histology revealed that BD cells were recorded exclusively in the dysgranular RSC, while HD cells were distributed across both granular and dysgranular RSC (**Fig. 2b** and **Supplementary Fig. 8**).

To test whether the bidirectional pattern was dependent on the rotated local visual cues, we recorded 12 BD cells in darkness: they maintained their bidirectional pattern (**Supplementary Fig. 9a–c**), suggesting that multimodal inputs can support the directionality of firing. Interestingly, nine BD cells recorded in an open field lost their bidirectional pattern (**Supplementary Fig. 9d**,**e**).

Unexpectedly, in addition to the 46 cells described above that reversed firing between compartments, which we named between-compartment BD (BC-BD) cells, we found 70 cells that expressed a bidirectional pattern *within* each compartment (**Figs. 2c** and **3a**,**b** and **Supplementary Fig. 10**). As before, detailed analyses ruled out that the within-compartment BD (WC-BD) cells could have been recording artifact. The doubled tuning curves were slightly asymmetric, with a dominant (slightly larger) peak that reversed direction between compartments (**Fig. 3c**), indicating a contributing influence of local landmarks. We examined whether WC-BD cells expressed two simultaneous tuning curves or a single curve that reversed frequently within compartments. Two tuning curves might result in increased overall spike count relative to HD cells (because the cells can fire in two directions instead of just one), while a single tuning curve that switched would result in lower and more variable firing rates

and a higher proportion of pauses in firing, producing long interspike intervals (ISIs). In fact, spike count was intermediate, being 37% higher than for HD cells and 42% higher than for BC-BD cells, both differences being significant (**Fig. 3d**). Firing rates did not differ for the three directional cell types, either for peak rates or mean rates (**Supplementary Table 3**). Also, the spread of firing rates was no different (**Fig. 3e**), and ISI analysis showed no increase in long intervals; moreover, analysis of the ISI histogram decay time-to-half-peak showed no difference between cell types (**Supplementary Table 3**). Taken together, these results suggest that WC-BD cells had true dual tuning curves, one slightly smaller, rather than single, periodically reversing curves.

What could cause this WC-BD pattern? It is likely due to the rat's previous experience of the two-compartment space and may reflect acquisition of new inputs from coactive HD cells during initial exploration (**Supplementary Fig. 11**). In our apparatus, because of the visual reversal, a landmark-driven BD cell would be coactive with two sets of HD cells having opposing firing directions. If these HD cells became additional new inputs due to Hebbian learning, the cell would then be driven to fire in both directions. This could explain why for WC-BD cells, one tuning curve was slightly stronger (because it has additional drive from the landmarks) and why this asymmetry was compartment-sensitive (**Fig. 3c**). In addition to evidence of interaction with the HD signal, we found evidence of spatially modulated activity in a very small subset of cells (**Supplementary Fig. 12**), suggesting a more general integrative role for this region.

What could be the function of BD cells? It may be to mediate both ways between visual landmarks and the global HD signal. A network of neurons having varying degrees of coupling between landmark-responsive cells and HD cells could use landmarks to compute head direction and, at the same time, use the HD signal to compute landmark stability; in this 'bootstrapping' manner, stable landmarks could be added to the constellation of inputs able to drive HD cells and unstable landmarks could be removed. This hypothesis is consistent with evidence from gene activation studies suggesting a role for dysgranular RSC in spatial tasks requiring light (i.e., vision) but not darkness[11,12]; human neuroimaging studies showing a role for RSC in monitoring landmark stability[4] and local reference frames[13], or integrating across scenes[14]; and from recording studies suggesting plasticity in the connections of landmarks to the HD network[15]. Thus, the network could function to learn which cues are the directionally stable ones that have a consistent relationship to the HD signal and so can act as landmarks to define a local directional reference frame.

METHODS

Methods, including statements of data availability and any associated accession codes and references, are available in the online version of the paper.

Note: Any Supplementary Information and Source Data files are available in the online version of the paper.

ACKNOWLEDGMENTS

This work was supported by grants from the Medical Research Council (G1100669) and Wellcome Trust (103896AIA) to K.J.

AUTHOR CONTRIBUTIONS

K.J. conceived the study and obtained funding; P.-Y.J. and K.J. designed the protocol; P.-Y.J. and D.O. performed surgeries and recordings; and P.-Y.J., L.S., G.C. and H.P. analyzed data. All authors interpreted data and discussed results. P.-Y.J. and K.J. wrote the manuscript. All authors commented on and edited the manuscript.

COMPETING FINANCIAL INTERESTS

The authors declare competing financial interests: details are available in the online version of the paper.

1. Taube, J.S. *Annu. Rev. Neurosci.* **30**, 181–207 (2007).
2. Taube, J.S. & Burton, H.L. *J. Neurophysiol.* **74**, 1953–1971 (1995).
3. Knierim, J.J., Kudrimoti, H.S. & McNaughton, B.L. *J. Neurosci.* **15**, 1648–1659 (1995).
4. Auger, S.D., Mullally, S.L. & Maguire, E.A. *PLoS One* **7**, e43620 (2012).
5. Chen, L.L., Lin, L.H., Green, E.J., Barnes, C.A. & McNaughton, B.L. *Exp. Brain Res.* **101**, 8–23 (1994).
6. Chen, L.L., Lin, L.H., Barnes, C.A. & McNaughton, B.L. *Exp. Brain Res.* **101**, 24–34 (1994).
7. Cho, J. & Sharp, P.E. *Behav. Neurosci.* **115**, 3–25 (2001).
8. Sugar, J., Witter, M.P., van Strien, N.M. & Cappaert, N.L.M. *Front. Neuroinform.* **5**, 7 (2011).
9. Taube, J.S., Muller, R.U. & Ranck, J.B. Jr. *J. Neurosci.* **10**, 436–447 (1990).
10. Yoganarasimha, D., Yu, X. & Knierim, J.J. *J. Neurosci.* **26**, 622–631 (2006).
11. Cooper, B.G., Manka, T.F. & Mizumori, S.J. *Behav. Neurosci.* **115**, 1012–1028 (2001).
12. Pothuizen, H.H.J., Davies, M., Albasser, M.M., Aggleton, J.P. & Vann, S.D. *Eur. J. Neurosci.* **30**, 877–888 (2009).
13. Marchette, S.A., Vass, L.K., Ryan, J. & Epstein, R.A. *Nat. Neurosci.* **17**, 1598–1606 (2014).
14. Robertson, C.E., Hermann, K.L., Mynick, A., Kravitz, D.J. & Kanwisher, N. *Curr. Biol.* **26**, 2463–2468 (2016).
15. Knight, R. *et al. Phil. Trans. R. Soc. Lond. B* **369**, 20120512 (2013).

ONLINE METHODS

Subjects. All procedures were carried out under the auspices of a Home Office license according to the Animals (Scientific Procedures) Act 1986. Nine adult male Lister Hooded rats weighing 300–350 g were individually housed under partial light-cycle shift (6 h) to allow recordings during their circadian dark cycle. They were mildly food restricted (to 90% free-feeding weight) and were weighed and checked daily.

Microdrives and surgery. Recordings were made using tetrodes, each composed of four twisted 25-µm or eight twisted 17-µm polyimide-coated platinum-iridium (90%/10%) wires (California Fine Wire, CA), attached to an Axona microdrive (Axona Ltd, Herts, UK). Under isoflurane anesthesia, the electrodes were chronically implanted in the left or right hemisphere. For four rats the electrodes were implanted in the RSC aimed at the granular subregion ($n = 1$ rat; coordinates in mm from Bregma: AP: −5.5, ML: ± 0.4, DV: 0.4) or dysgranular subregion ($n = 3$ rats; AP: −5.5, ML: ± 1.0, DV: 0.4). For three rats the electrodes were aimed at postsubiculum (AP: −7.5, ML: ± 3.2, DV: −2.0) and for two rats they were aimed at the anterodorsal thalamic nucleus (ADN; AP: −1.8, ML: ± 1.4, DV: −3.9). After the surgery, rats received meloxicam mixed with condensed milk for 3 d for postoperative analgesia and were given at least 7 d to recover before the experiment began.

Apparatus. The recording apparatus (**Supplementary Fig. 1a**) was a 120 × 120 cm square box with 60-cm high walls, isolated from the rest of the room by a cylindrical floor-to-ceiling curtain 260 cm in diameter. The box was divided into two equal rectangular subcompartments by a 60-cm high wall, in the center of which was an aperture, 10 cm at the base and 15 cm at the top, which allowed free movement between compartments. The compartments were each polarized by a 20-cm wide × 40-cm high plastic white cue card attached to the short wall and located to the left when facing the doorway. Walls and floor were covered with black vinyl sheets, allowing the experimenter to wipe each compartment with a sponge moistened with lemon or vanilla food flavoring so as to allow the rat to distinguish the compartments. Six circularly arranged ceiling lights lighted the box and a nontuned radio was fixed to the ceiling in a central position relative to the box, producing a background noise > 70 dB to mask uncontrolled directional sounds. For recordings made in darkness, the cue cards were removed so as to minimize focal olfactory/tactile landmarks.

Recording setup and procedure. For recording, the microdrive connector was attached to the headstage and recording cable, through which the signals from each wire were amplified, filtered, digitized (48 kHz) and stored by an Axona DacqUSB acquisition system. Spikes were amplified 3,000–5,000 times and bandpass-filtered between 0.8 and 6.7 kHz; local field potential (LFP) signals were amplified 1,000 times and filtered between 0 and 475 Hz. Two light-emitting diodes (LEDs), one large and one small and separated by 5 cm, were attached to the headstage assembly to provide the position and the orientation of the rat's head. The LEDs were imaged with an overhead camera at a sampling rate of 50 Hz.

Beginning 1 week after surgery, the animals were screened daily for single-unit activity. Screenings were made in a small box, outside the curtain. Tetrodes were lowered 50 µm if no single-unit activity was found or after a complete recording session. When a set of units was isolated, the animal was transferred to the experimental apparatus inside the curtained area and a sequence of five recording trials was run, as follows:

- Trial 1 (baseline): The orientation of the box was random with respect to the outside room. Rats were placed in one of the compartments, facing in a randomly determined direction. For two RSC-implanted rats, starting compartments were initially the same for every trial, but then switched to being randomly selected. For the remaining two RSC-implanted rats it was always random. For 10 min the animals freely moved between compartments, foraging for cooked sweetened rice thrown in sporadically by the experimenter.
- Trial 2 (rotated baseline): As in trial 1 but the box was randomly rotated by 45°, 90° or 180°, clockwise or counterclockwise, to check local cue control of directional firing.
- Trial 3 (door-closed odor 1): The apparatus was again arbitrarily rotated and the animal placed in one of the compartments (randomly chosen). The connecting door was closed so the rat was confined to that compartment for a 5-min trial. This was to see whether the odor cues alone were enough to reinstate the correct orientation of firing.
- Trial 4 (door-closed odor 2): The apparatus was rotated and the rat recorded in the other compartment for 5 min.
- Trial 5 (baseline): A last standard 10-min door-open trial was run with the apparatus having the same orientation as in trial 1.

Between trials, animals were removed from the apparatus and placed in a box in a random location outside the curtain for 2 min, to let the experimenter manipulate the box (rotating the apparatus and/or closing or opening the door). The animal was then mildly disoriented by rotating its holding box before the next trial.

For some recording sessions, two 10-min darkness trials were added after trial 5. For the first of these (trial 6: darkness), animals were not removed from the box after trial 5, but the computer screen and ceiling lights were turned off before recording began. After this trial, the animal was removed, the box randomly rotated and the rat mildly disorientated before the last darkness trial (trial 7: rotated darkness).

Data analysis. Data collection and analysis were not performed blind to the conditions of the experiments.

Spike sorting was performed manually using the graphical cluster-cutting software Tint (Axona) with the help of an automated clustering algorithm (Klustakwik 3.0)[16]. Units having interspike intervals < 2 ms (refractory period) were removed due to poor isolation, as were cells with a peak firing rate ≤ 1 Hz. To prevent repeated recordings of the same cell over days, clusters that recurred on the same tetrodes in the same cluster space across recording sessions were only analyzed on the first day.

The rat's head direction was calculated for each tracker sample from the projection of the relative position of the two LEDs onto the horizontal plane. The directional tuning for each cell was obtained by dividing the number of spikes fired when the rat faced a particular direction (in bins of 6°) by the total amount of time the rat spent facing that direction. The peak firing rate was defined as the rate in the bin with the highest rate; the cell's preferred firing direction was defined as the angle of this bin.

Directionality analysis. Rayleigh vectors were used to assess directional specificity, with significant directionality being assigned to cells whose Rayleigh vector score exceeded the 99th percentile of a control distribution. For the control procedure, for each cell's trial 1 data, we shifted the time of every spike by a uniform amount, chosen randomly from between 20 s and (recording duration − 20) s; this was repeated 400 times per cell (1,090 cells × 400 = 436,000 rotations). The 99th percentile value came to 0.26, similar to that reported in previous HD cell studies[17,18]. Thus, all cells for which the Rayleigh vector length was greater or equal to 0.26 and for which the firing rate exceeded 1 Hz were classified as HD cells. The cells selected for the study were required to reach selection criteria in both trials 1 and 5.

Because of the unexpected observation of cells that fired in two opposing directions, we adapted the above directionality analysis by using an angle-doubling procedure in which the heading angle of each spike was multiplied by two and the results plotted modulo 360°: this has the effect of converting a BD distribution to a unimodal one, from which the population of directionally firing neurons could be selected using the 99th percentile criterion, computed as before, which was equal to 0.22.

We tested whether all 360° of compass heading were represented in the directional cells we recorded by referencing the firing direction of each cell to the lemon-compartment orientation in trial 1 and determining the nonuniformity of the distribution of angular distances with a Rayleigh test.

Selection of BD cells. We selected BD cells by defining a 'flip score' above which cells were considered bidirectional. Flip scores were calculated with an autocorrelation procedure, by rotating the polar firing rate plot in steps of 6° and calculating the correlation between the rotated and unrotated plots at each step. The bidirectional pattern was apparent as a sinusoidal modulation of this autocorrelation with a peak at 180° (**Supplementary Fig. 4**). The flip score for each cell was defined as the difference between the correlations at the expected peak (180°) and the expected troughs (90°). For the entire population of directional cells this yielded two clusters (**Fig. 2** and **Supplementary Fig. 4**), the local minimum between which (value of 0.6) was used to separate BD from HD cells.

doi:10.1038/nn.4465

BD cells selected for the study were those that exceeded the vector length and flip score criteria in both trials 1 and 5.

Cell-isolation analyses. Cell-isolation analyses were performed to rule out the hypothesis that BD cells were really two co-recorded classic HD cells with opposing tuning curves. This was done in three different ways, as follows:

(1) Cluster space analysis (**Supplementary Fig. 5a**). This analysis sought to establish that the clusters from the spikes belonging to the two individual tuning curves of BD cells were no further apart than the clusters of clearly unidirectional HD cells arbitrarily divided in two. This was based on scatterplots of the key waveform clustering parameter, which was peak–trough amplitude. For BD cells, we extracted two subclusters containing spikes emitted in the 180° range surrounding each tuning curve peak, found their centers of mass (CoM) in the scatterplot cluster-space and calculated the distance between the two CoMs. Results were compared to a control data set comprising the spikes from HD cells that had been randomly allocated to one or the other of two subclusters; we then calculated the distance between the CoMs of these. This procedure was repeated 2,000 times per cell. Data from the BD cells and the control data were compared with a two-sample *t*-test.

(2) In a second analysis (**Supplementary Fig. 5b**), we calculated the probability that failure to separate the clusters of HD cells would have resulted in tuning-curve pairs that just happened to be 180° apart. To do this we randomly (with replacement) selected pairs of HD cells from the total pool 10,000 times, and for each pair we cross-correlated the tuning curves and derived the angle of the highest correlation. Then, we calculated the percentage of cells with an angular distance at 180 ± 12° (corresponding to two bins of 6°) and compared this, using a chi-squared test, with the observed data.

(3) In the last analysis, we computed the Pearson's correlation coefficient between firing rates for the two tuning curves (**Supplementary Fig. 5c**); if these were from different cells then the rates should be no more correlated than those of any two randomly selected cells. The correlation value was compared to control correlations generated by randomly selecting, with replacement, 10,000 pairs of HD cells.

Directionally color-coded spatial spike maps. Directional color-coded spike maps were constructed in order to visually display the spatial distribution of directional activity. We first defined a color map with a circular gradient of color ranging in 90° bins from blue to green to red to yellow (**Fig. 1b**). For each cell, we aligned the direction of blue in the color map with the peak firing bin in trial 1, with all other directions being colored accordingly, and assigned each spike the appropriate color based on its associated head direction. We then generated a spatial spike plot by smoothing the path of the rat in 20-ms bins and overlaying it at the appropriate places with the color-coded spikes.

Compartmental analysis. Some neurons had bidirectional tuning curves even in individual subcompartments of the apparatus, and we investigated whether these behaved like HD cells that periodically reversed their tuning curve direction or more like cells with simultaneous, opposing tuning curves. Analysis was performed on the two tuning curves for the whole apparatus and also for each individual compartment on the baseline trial. We identified epochs in the recording trial when the rat faced continuously in the direction (± 45°) of one or other tuning curve, and then within these epochs we computed the firing rate (number of spikes divided by epoch duration) and firing rate spread (s.d. of firing rates across epochs).

Directional activity in darkness and in the open field. Directionally modulated cells were recorded in darkness to determine whether activity was maintained between light and dark trials. For each cell we computed (i) the vector length and the flip score as described previously and (ii) the Pearson correlation coefficient of each cell's directional firing rates between continuous light–dark trials 5 and 6, and between the two dark trials 6 and 7, and compared them using a Kruskal-Wallis nonparametric test.

Nine BD cells were additionally recorded in a 120 cm × 120 cm open field after five experimental recording sessions. For each BD cell, we calculated the vector length and the flip score to investigate whether they shared directional properties found in the two compartment apparatus.

Spatial rate maps and spatial correlation analysis. Spatial rate maps were generated by dividing the two-compartment apparatus into an array of 40 × 40 square bins, each 3 × 3 cm in size. Spikes per bin were divided by time spent in that bin to provide a firing rate (Hz). Smoothed firing rate maps were then generated using a boxcar procedure in which the firing rate in each bin was replaced by that of the mean of itself plus the immediately surrounding bins (eight surrounding bins for central bins, five for edge bins and three for corner bins). In both raw and smoothed rate maps, pixels that were not visited by the rat were displayed in white. The firing rate of the cell was color-coded from low (light blue) to high (dark red).

Spiking characteristics. For recordings from the three brain areas, we looked at spiking characteristics for the five cell types (PoS HD, ADN HD, RSC HD, RSC BC-BD and RSC WC-BD) including peak firing rates and ISI histograms.

For the ISI analysis, a histogram of ISIs with 2-ms bins was generated for each cell type, and the peak was taken as the center of the bin with the highest count. Inspection of the ISI histograms suggested different decay times for the different cell types so we calculated decay time by fitting to the histogram a one-term exponential decay function of the form $y = ae^{(bx)}$ from the peak to (peak + 1) s, using the 'fit' function from Matlab's Curve Fitting Toolbox. Time to half-peak was then taken as the time taken for the exponential fit to decay to half the peak value.

For retrosplenial WC-BD, BC-BD and HD cells, ISIs were also considered only for time periods during which head direction was within ± 45° of the preferred firing direction of the cell. For HD cells, this was taken as the location of peak firing rate in the polar plot. For BD cells, this same method was used to find one preferred firing direction, and then the other peak was found using a circular autocorrelation. For the exponential curve-fitting, the lowest-spiking 25% of all cells were excluded (those with fewer than 145 spikes occurring within ± 45° of the peak direction for that cell).

Statistics. No statistical methods were used to predetermine sample sizes, but our sample sizes are similar to those reported for HD cells in previous studies[7,9,10]. Statistical tests included Student's *t*-tests, ANOVA, Pearson's correlations, chi-square tests, Rayleigh tests, Mann-Whitney *U*-tests, Kruskall-Wallis tests and circular *V*-tests. Data distribution was assumed to be normal, but this was not formally tested. A **Supplementary Methods Checklist** is available.

Histology. At the completion of the experiment, rats received an overdose of pentobarbital and were perfused intracardially with 0.9% saline followed by 4% formaldehyde. The brains were removed, stored for 1 d in formaldehyde and then in 30% sucrose solution until the brains sank (24–48 h). After this they were frozen with dry ice and sliced into 30-µm-thick sections: coronally for ADN and RSC animals and sagittally for PoS animals. The sections were mounted on glass slides and stained with cresyl violet or thionine. The positions of the tips of the electrodes were determined from digital pictures, acquired with an Olympus microscope (Olympus Keymed, Southend-on-Sea, UK) and imported into an image manipulation program (Gimp 2.8, distributed under a General Public License). Recording sites were determined by measuring backwards from the deepest point of the track and identified with the help of the rat brain atlas from Paxinos and Watson[19].

Data availability. The raw and analyzed data that support the findings of this study are available at https://dx.doi.org/10.14324/000.ds.1529898.

16. Kadir, S.N., Goodman, D.F.M. & Harris, K.D. *Neural Comput.* **26**, 2379–2394 (2014).
17. Bonnevie, T. *et al. Nat. Neurosci.* **16**, 309–317 (2013).
18. Giocomo, L.M. *et al. Curr. Biol.* **24**, 252–262 (2014).
19. Paxinos, G. & Watson, C. *The Rat Brain in Stereotaxic Coordinates*, 6th edn. (Elsevier Academic Press, 2007).